Current Optics and Photonics
Vol. 1, No. 5, October 2017, pp. 529-537

ISSN: 2508-7266(Print) / ISSN: 2508-7274(Online)
DOI: https://doi.org/10.3807/COPP.2017.1.5.529

# Correlation of Peak Time Shift in Blood Pressure Waveform and PPG Based on Compliance Change Analysis in RLC Windkessel Model

**Wonsuk Choi[1] and Jin-Ho Cho[2]***

[1]*Graduate School of Electronics Engineering, College of IT Engineering, Kyungpook National University, Daegu 41566, Korea*
[2]*School of Electronic Engineering, College of IT Engineering, Kyungpook National University, Daegu 41566, Korea*

(Received July 29, 2017 : revised September 1, 2017 : accepted September 11, 2017)

We explored how changes in blood vessel compliance affected the systolic rise time (SRT) of the maximum blood pressure (BP) peak wave and the diastolic fall time (DFT) of the minimal BP peak wave, compared to photoplethysmograpic (PPG) parameters, using a two-compartment, second-order, arterial Windkessel model. We employed earlier two-compartment Windkessel models and the components thereof to construct equivalent blood vessel circuits, and reproduced BP waveforms using PSpice technology. The SRT and DFT values were obtained via circuit simulation, considering variations in compliance (the dominant influence on blood vessel parameters attributable to BP changes). And then performed regression analysis to identify how compliance affected the SRT and DFT. We compared the SRTs and DFTs of BP waves to the PPG values by reference to BP changes in each subject. We confirmed that the time-shift propensities of BP waves and the PPG data were highly consistent. However, the time shifts differed significantly among subjects. These simulation and experimental results allowed us to construct an initial trend curve of individual BP peak time (measured via wrist PPG evaluations at three arm positions) that facilitated accurate individual BP estimations.

*Keywords* : Blood pressure estimation, PPG, Systolic rising time, Compliance, Blood pressure wave
*OCIS codes* : (170.1470) Blood or tissue constituent monitoring; (170.3660) Light propagation in tissues; (170.3890) Medical optics instrumentation; (170.0170) Medical optics and biotechnology

## I. INTRODUCTION

Real-time portable BP measurement using a simple, continuous, cuffless technique, without restraining the patient, is of great interest to both clinicians and the general public [1-3]. Various methods [4], for example, employing pulse transit time (PTT) which is the time between the R wave of an electrocardiogram (ECG) and the peak of photoplethysmograpic (PPG) have attracted much attention, due to allowing BP estimation without use of a BP cuff. However, the method is inconvenient [5-7] in that electrographic signals from the chest or arm are required, electrodes must be attached, and a PPG detection device must be affixed to a finger. Since the PPG is a noninvasive signal obtained very conveniently from finger or wrist, many researchers have studied the relationship between the PPG and blood pressure [8-11].

Recently, Teng, and Yoon et al., [12-14] have developed methods whereby BP can be estimated using only BP pulse waves or PPG skin signals.

Woo et al. [13] described a method that does not use either a cuff or an ECG electrode. This method measures the central BP accurately; the standard deviation is 4.7 mmHg. The transmission of radial artery pressure to a sensor on the surface of the wrist is measured electro-mechanically. However, because the pulsation spot of wrist is relatively small, it is difficult to obtain continuous, stable pressure signals. Thus, it is better to estimate BP by

*Corresponding author: jhcho@ee.knu.ac.kr

Color versions of one or more of the figures in this paper are available online.

measuring the amplitude of blood flow signals from the ulnar or radial artery of the wrist using a PPG sensor rather than a watchband-type pressure sensor. However, Elgendi [16] emphasized that the PPG signal is normalized via automatic gain control (AGC) during amplification, and the absolute amplitude thus correlates rather poorly with the BP. To check the effectiveness of PPG-derived BP measurements, Rohan et al. [15] and Yoon [14] measured the SRTs and diastolic falling times (DFTs) of PPG BP parameters in five subjects and compared the results with those of conventional sphygmomanometry. Yoon found that the SRT decreased, and the DFT increased, when the BP rose, and the correlation coefficients of BP with SRT and DRT were only 0.60 and 0.76, respectively. However, the reason why a PPG time shift developed as the BP changed remained unclear.

Westerhof and others have sought to estimate BP via vascular modeling [17-19]. Patrick upgraded a conventional two-element Windkessel model with RC alone to a four-element model, allowing evaluation of the dicrotic portions of reflection waves in arterial BP waveforms [20]. However, the effects of such changes on SRT and DRT measurements were not evaluated.

Woo et al. [13] estimated blood pressure (BP) by reference to the wrist pressure waveform, and obtained more accurate results than did Yoon et al. [14-15] employing a PPG approach. To increase the reliability of BP estimation via PPG methods, it is essential to measure individual parameters accurately by reference to blood vessel modeling. In addition, the parametric BP waveform should be examined to determine whether the PPG waveform can be used to this end, rather than the pulse BP. Among the various mechanical features of blood vessels, the most important parameter affecting the BP or PPG waveform would be expected to be compliance, because a change in BP directly affects vessel wall tension. Therefore, different from previous studies [12-14], to increase the accuracy of BP estimation from PPG waveforms, changes in the compliance of individual blood vessels should be measured accurately using a two-compartment Windkessel model.

Here, we explored how changes in blood vessel compliance modulated PPG parameters. We explored the effects of such changes on the SRT and DFT using a two-compartment Windkessel model and published data. We constructed a blood vessel circuit, reproduced the BP waveform employing p-spice software, and explored the effects of changes in compliance. To verify the validity of the parameters used in the simulation, we created a circuit generating BP waveforms using the estimated RLC values, and compared this with the original BP waveform. We measured the timing of the systolic and diastolic peaks when the compliance changed, and applied regression analysis to explore the relationships between these times and compliance. We compared the SRT and DFT of the BP wave and the PPG parameters associated with three arm positions (up, flat, and down). The times elapsed between the two signals were in good agreement. The time shifts varied notably among subjects. Therefore, based on our simulations and the experimental data, we found that BP estimation, using the personal based trend curve obtained by regression analysis of the peak time shifts in wrist PPG parameters at the three arm positions of each subject, improved the accuracy of BP estimation.

## II. METHODS

### 2.1. BP Waveforms and PPG Parameters of the Brachial Artery

Figure 1(a) shows a BP waveform measured immediately above the radial artery of an adult using a pressure sensor with a cuff (SS-19L; Biopac Systems Inc.) placed above the wrist radial artery and Fig. 1(b) the PPG skin signal yielded by a wrist PPG sensor (PSL-iPPG, Physio Lab) at the same point.

As shown in Fig. 1, the BP and PPG pulse waveforms were very similar. This is because the PPG waveform reflects the change in blood vessel volume attributable to the BP change. Both waveforms have two components. The pulse wave includes the rising edge of the systole phase and the falling edge of the diastole phase. In the diastole phase, a dicrotic notch is created via reflection from the periphery. When the LED illuminates the blood vessel, the PPG waveform is generated by intensity modulation of the light attributable to BP changes. The PPG data thus reflects the BP. However, the details of the relationship between the PPG and BP signals remain unclear. No commercial cuffless device that continuously monitors BP is yet available. It is thus important to accurately derive pressure-related parameters from PPG waveforms.

We investigated the relationships between PPG parameters and blood vessel compliance (the pressure wave) of the brachial artery with the aid of dynamic modeling.

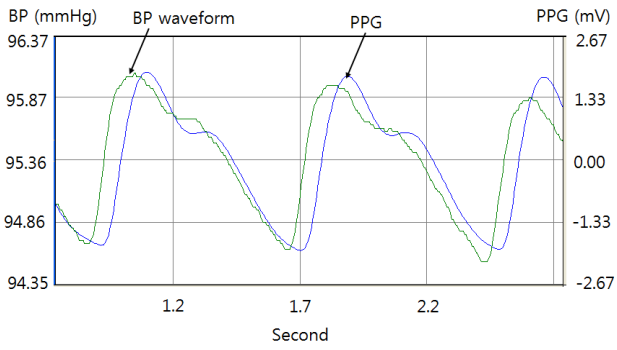


FIG. 1. Pressure and photoplethysmographic (PPG) waveforms of the brachial artery: (a) BP waveform; (b) PPG waveform.

### 2.2. BP Modeling Using a Two-compartment Windkessel Model

The Windkessel model is the simplest circuit representing the human cardiovascular system, incorporating peripheral resistance and vascular compliance using the electrical components R (fluid resistance) and C (compliance). The model has been used to estimate human BP [21]. Others employed an RLC Windkessel model (L: inertance) that features two different reservoirs, inertance, and two resistances; the model explains the dicrotic phenomenon shown in Fig. 2 [22, 23]. Figure 2(a) shows a two-compartment model of the arterial circulatory system and Fig. 2(b) shows the electrical analog thereof, derived using the RLC components. Is represents the aortic blood flow; C1 and C2 are the compliances (the blood vessel reservoirs before and after the sample length Δl, respectively); L is the inertance (the mass of the blood flow); Ra is the fluid resistance of the blood vessel; and R is the fluid resistance of the capillary bed.

The model yields an RLC estimation equation by deriving voltage and current node equations and then solving the state variable. The details are described in reference [22].

### 2.3. Parameters Extracted from the BP Waveform

It is important to extract parameters using the RLC Windkessel approach to model the actual BP waveform, and then to examine the influence of changes in specific parameters on the BP. To this end, various components were extracted from the actual BP waveform of the brachial artery of a normal adult [23], as shown in Fig. 3. The heart beat pulse is 1.23 Hz, the cycle is 0.814 s, the systolic time is 0.314 s, and the diastolic time is 0.5 s. The procedure used to create an RLC model for the vessel is as follows: the values are derived at eight different points and the data for each point are curve-fitted using MATLAB, yielding a waveform equation very similar to the original waveform (Fig. 4).

The estimated RLC values for the waveform equation are listed in Table 1. These values were used to construct

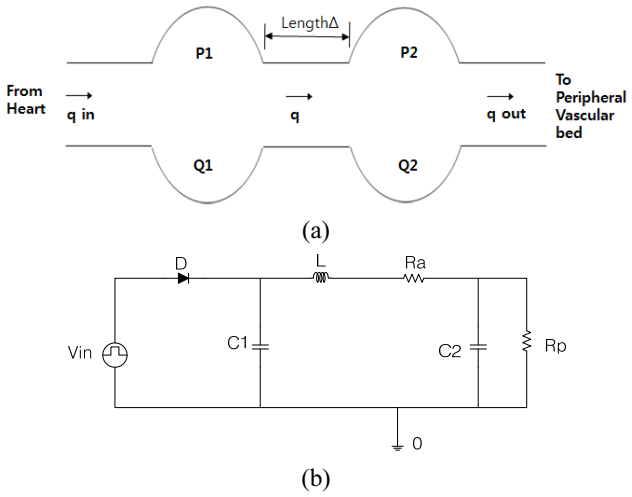


FIG. 2. (a) Two-compartment physical model of the arterial circulatory system. (b) The RLC Windkessel model.

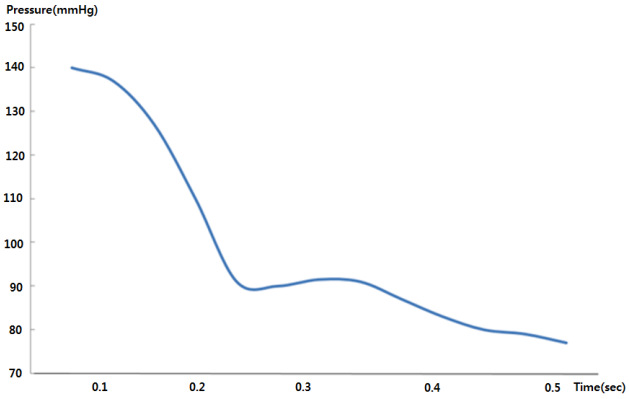


FIG. 3. In the human brachial artery, the abscissa is 1.23 Hz, the cycle is 0.814 s, the systole is 0.314 s, and the diastole is 0.5 s [23].

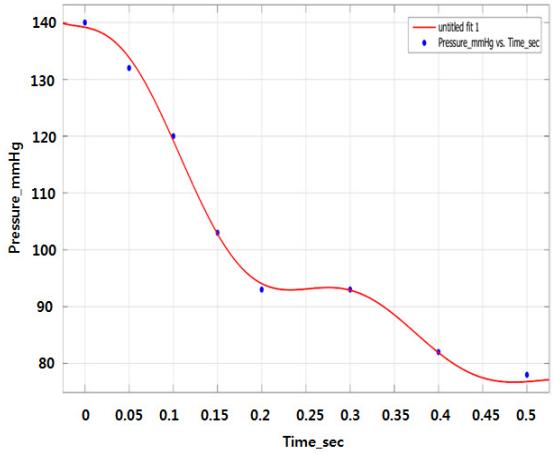


FIG. 4. The curve-fitting graph (BP=140/80 mmHg).

TABLE 1. The *RLC* values for the circuit of Fig. 5

| | |
|---|---|
| R | 1000 Ω |
| C1 | 867 μF |
| C2 | 867 μF |
| L | 29.05 H |

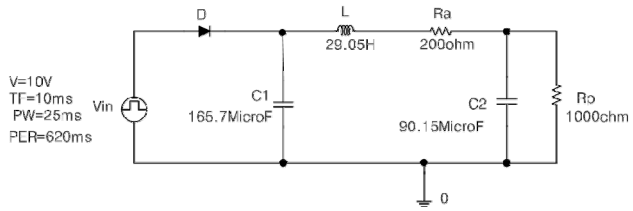


FIG. 5. The calculated RLC-based equivalent circuit.

a two-compartment Windkessel circuit using PSpice, as shown in Fig. 5. The input signal was a rectangular pulse equivalent to the pressure in the left ventricle when pumping.

### 2.4. Simulation of Peak Time Shifts in the SRT and DFT Using the Extracted Parameters

In general, arterial BP is influenced by the RLC parameters. The BP waveform is affected predominantly by the compliance (C) of the vessel wall. This is because a change in BP alters the tension at the blood vessel wall; the change in compliance is the reciprocal of vessel stiffness. Also, as the total blood volume remains unchanged when the arterial BP varies, the inertance L associated with the mass of blood flow per unit length of the blood vessel will not change significantly. Muscle compliance is controlled autonomically, and affects blood vessel resistance. However, we assume here that the parameter exerting the greatest effect on the BP waveform is exerted by blood vessel compliance. Both the C1 and R components of the two-compartment Windkessel model influence the exponential decay time after systole of the output BP waveform, and C2 greatly affects the vibration characteristics of the dicrotic notch region [20].

A simulation created using the circuit of a two-compartment Windkessel model is shown in Fig. 5. The simulation employed the parameters listed in Table 1, and both the SRT and DFT changed when the C values were varied. Changes in compliance greatly affected the times at which the systolic and diastolic peaks appeared, and the amplitude of the BP waveform in the region of the dicrotic notch. Figure 6 shows how a change in BP waveform shifts the SRT and DFT; the four compliance changes from the original value are shown in four different colors. When the compliance increased, the SRT also rose and the DFT tended to decrease. In the Figure, L and R are fixed, and the red, blue, purple, and light-blue BP waveforms are those corresponding to compliances of 167, 210, 290, and 350 μF, respectively.

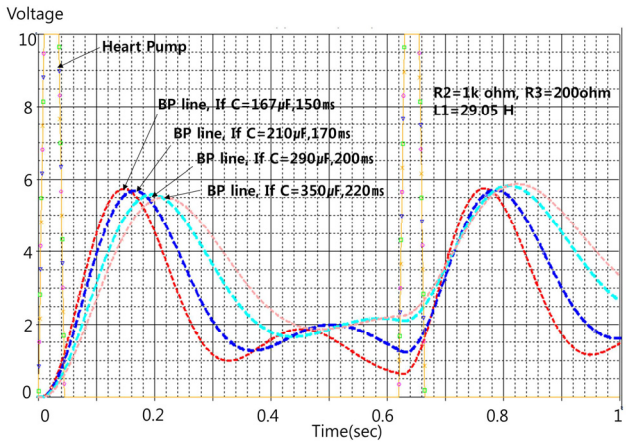


FIG. 6. Arterial BP waveforms created using the electrical analog model, with variations in compliance.

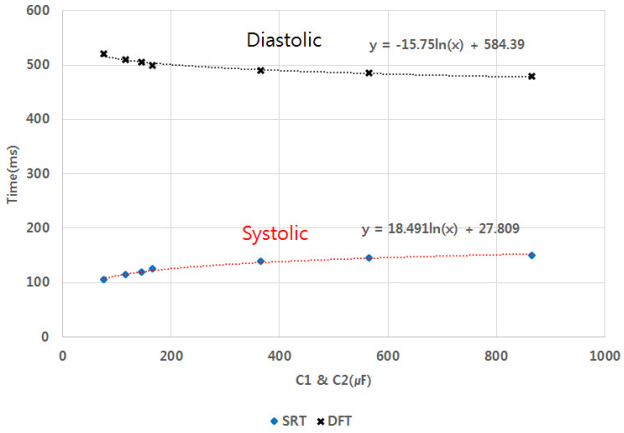


FIG. 7. Changes in the systolic rising time (SRT) and diastolic falling time (DFT) as blood vessel compliance varies.

Figure 7 shows the trend line obtained by measuring SRT and DFT using the compliances listed in Fig. 6. The points where SRT and DFT shift at various C values fell on a gentle saturation curve (Fig. 7). The relevant equations are:

$$S(t) = 18.491\,ln(x) + 27.809 \quad (1)$$

$$D(t) = -15.75\,ln(x) + 584.39 \quad (2)$$

Equations (1) and (2) show that the SRT [S(t)] and DFT [D(t)] are saturated, and increase as a function of their natural logarithms with increasing compliance (x), consistent with general vascular behavior. As compliance increases, the SRT peak increases and the DFT peak decreases; the reverse occurs as compliance decreases. This is because, as arterial BP increases, the blood vessel tension also rises, reducing compliance and the SRT but increasing the DFT. If the BP falls, the opposite is true. Clearly, such findings can be used to estimate the BP objectively by reference to PPG parameters.

### 2.5. Measurement of the SRT and DFT of the BP Wave According to the BP

We have shown how modeling and simulation reveal changes in the SRT and DFT as the BP varies. A prerequisite was that any change in the SRT would be evident in the pressure waveform of the brachial artery. However, it is very difficult to obtain reliable BP waves from a pressure sensor on the wrist brachial artery (including the radial and ulnar arteries).

Therefore, in this paper, we measured the wrist PPG waveform rather than pressure pulse waves to measure the peak time shifts of BP waves. However, it was essential to confirm that the SRT and DFT revealed by PPG waveforms were similar to those of the BP waves. Thus, we measured BP waves and PPG waveforms simultaneously in 10 subjects, and compared them. The systolic and diastolic BP, and the BP wave and PPG parameters, were measured with the arms held flat, up, and down (in that order). All

subjects were healthy males aged 22-34 years. BP waves were measured using a digital electronic manometer (Hem-7120; OMRON) and real-time BP waveforms were created, using a pressure sensor integrated into a cuff (SS19L; Biopac Systems Inc.), placed over the wrist ulnar artery, at a pressure of 80 mmHg. The output waveforms were transferred to a PC; then, the cuff removed, and the radial artery PPG waveforms were measured with the aid of the PSL-iPPG module (Physio Lab). The peak time of each subject's PPG was obtained with the aid of a memory oscilloscope (GDS3252; Tektronix).

## III. RESULTS & DISCUSSION

### 3.1. The SRTs and DFTs of the BP Waveforms

Table 2 shows the BPs of the 10 subjects. The values measured with the arms up, flat, and down were inversely proportional to the SRT and DFT of the BP wave. The peak times are the averages of eight successive BP measurements taken in each arm position. The BP differences when the arms were angled differently averaged 20-30 mmHg. Thus, the SRTs and DRTs also varied (by 20-60 ms), consistent with the simulation data obtained when compliance was varied in the two- compartment Windkessel model.

### 3.2. SRTs and DRTs Yielded by the PPG Signals by Reference to BP

Using the BP waves measured by the pressure sensor, the PPG SRTs and DFTs were detected, averaged, and plotted against the manometric BP values to obtain a trend curve for each subject.

Table 3 shows the results when the arms were in the up, flat, and down positions. The PPG SRT and DFT changes

TABLE 2. The SRTs and DFTs of the BP waveforms (n=10) measured at each of three arm positions

| No. (N=10) | Subject | Arm up | | | Arm flat | | | Arm down | | |
|---|---|---|---|---|---|---|---|---|---|---|
| | | SRT (ms) | DFT (ms) | BP mmHg (sys/dia) | SRT (ms) | DFT (ms) | BP mmHg (sys/dia) | SRT (ms) | DFT (ms) | BP mmHg (sys/dia) |
| 1 | A | 165 | 530 | 87/51 | 158 | 537 | 141/99 | 148 | 547 | 151/113 |
| 2 | B | 256 | 639 | 97/63 | 161 | 734 | 130/90 | 112 | 783 | 151/113 |
| 3 | C | 215 | 537 | 93/72 | 205 | 547 | 129/94 | 190 | 562 | 146/105 |
| 4 | D | 215 | 515 | 72/45 | 205 | 525 | 124/79 | 155 | 575 | 150/106 |
| 5 | E | 255 | 527 | 95/68 | 210 | 572 | 141/105 | 150 | 632 | 159/115 |
| 6 | F | 220 | 557 | 76/37 | 195 | 582 | 107/75 | 140 | 637 | 120/80 |
| 7 | G | 180 | 480 | 65/42 | 105 | 555 | 105/75 | 90 | 570 | 128/94 |
| 8 | H | 173 | 567 | 90/60 | 148 | 592 | 130/99 | 130 | 610 | 142/111 |
| 9 | I | 190 | 550 | 68/46 | 160 | 580 | 118/94 | 115 | 625 | 141/111 |
| 10 | J | 165 | 575 | 58/37 | 155 | 585 | 110/83 | 140 | 600 | 130/93 |

SRT, systolic rising time; DFT, diastolic falling time; BP, blood pressure; sys, systole; dia, diastole

TABLE 3. The PPG SRTs and DFTs (N=10) measured at each of three arm positions

| No (N=10) | Subject | Arm up | | | Arm flat | | | Arm down | | |
|---|---|---|---|---|---|---|---|---|---|---|
| | | SRT (ms) | DFT (ms) | BP mmHg (sys/dia) | SRT (ms) | DFT (ms) | BP mmHg (sys/dia) | SRT (ms) | DFT (ms) | BP mmHg (sys/dia) |
| 1 | A | 145 | 550 | 87/51 | 137 | 558 | 141/99 | 129 | 566 | 151/113 |
| 2 | B | 237 | 658 | 97/63 | 230 | 665 | 130/90 | 126 | 769 | 151/113 |
| 3 | C | 210 | 542 | 93/72 | 195 | 557 | 129/94 | 175 | 577 | 146/105 |
| 4 | D | 220 | 510 | 72/45 | 200 | 530 | 124/79 | 170 | 560 | 150/106 |
| 5 | E | 255 | 527 | 95/68 | 187 | 595 | 141/105 | 150 | 632 | 159/115 |
| 6 | F | 218 | 559 | 76/37 | 195 | 582 | 107/75 | 155 | 622 | 120/80 |
| 7 | G | 160 | 500 | 65/42 | 154 | 506 | 105/75 | 110 | 550 | 128/94 |
| 8 | H | 207 | 533 | 90/60 | 150 | 590 | 130/99 | 122 | 618 | 142/111 |
| 9 | I | 196 | 544 | 68/46 | 150 | 590 | 118/94 | 125 | 615 | 141/111 |
| 10 | J | 175 | 565 | 58/37 | 164 | 576 | 110/83 | 124 | 616 | 130/93 |

SRT, systolic rising time; DFT, diastolic falling time; BP, blood pressure; sys, systole; dia, diastole

were inversely proportional to the BP, and thus were similar to the BP waveform data and consistent with the simulations described above.

The BP time shifts of subject A are shown in Fig. 8. The black dotted, long-dashed, and dashed lines represent the PPG, BP wave, and average diastolic time, respectively. The red dotted, long-dashed, and dashed lines represent the PPG data, BP wave, and average systolic time, respectively. The lines were obtained using the regression routine of MS Excel (Microsoft Corp.). The shifts in the SRT and DFT were very similar to those of the BP waveforms (Table 2). The correlation coefficients between the trend line data of the BP waveforms and the PPG time shifts are summarized in Table 4 for each arm position, which reveals similarities between the BP waveforms and PPG data of all 10 subjects; we averaged the figures of Tables 2 and 3. The degree of similarity was high, at; 0.881 for the systolic, and 0.889 for the diastolic, waveform. There-

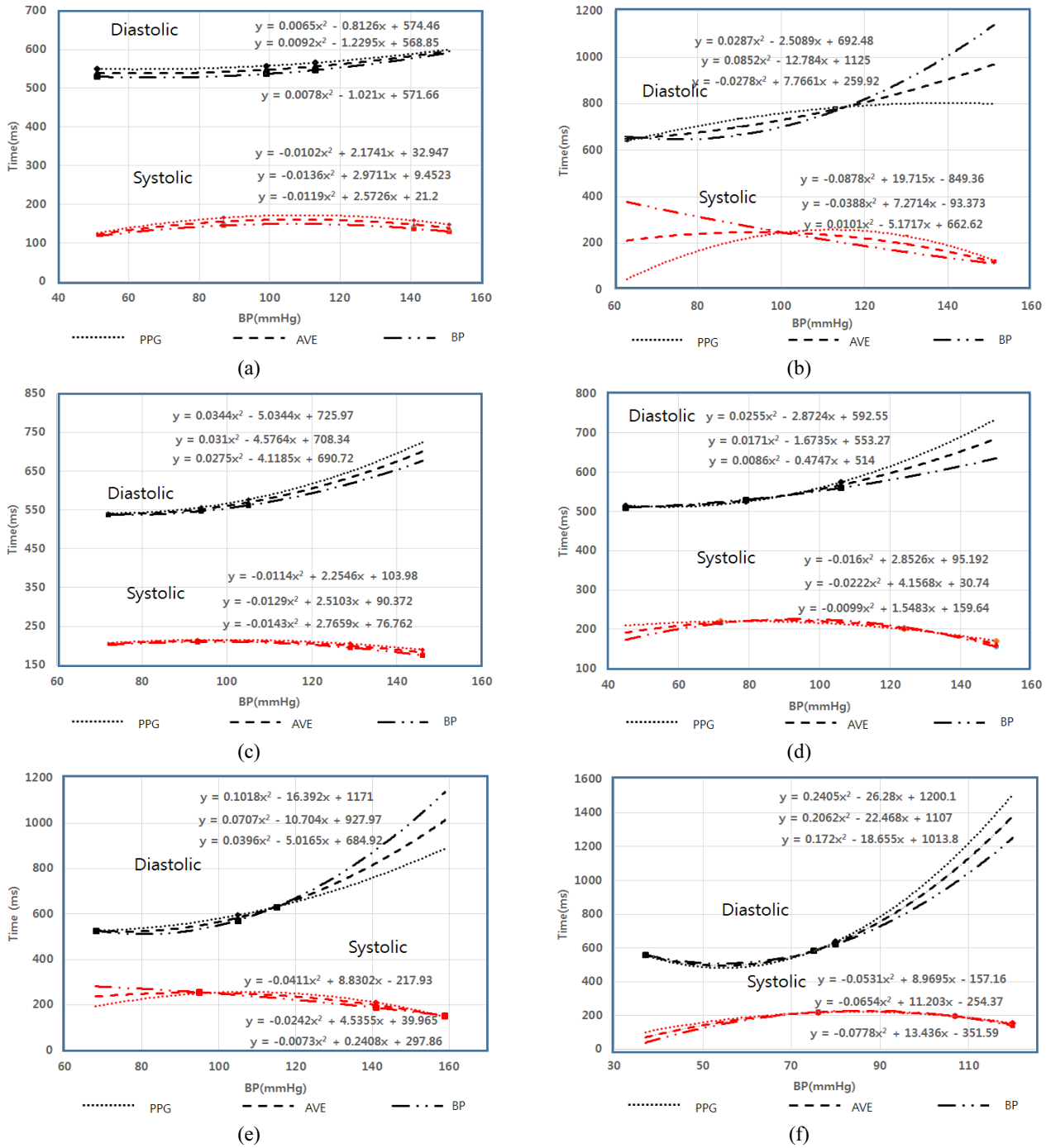


FIG. 8. Comparison of the time shifts (SRT, DFT) in the BP waveform and PPG data of subject A.

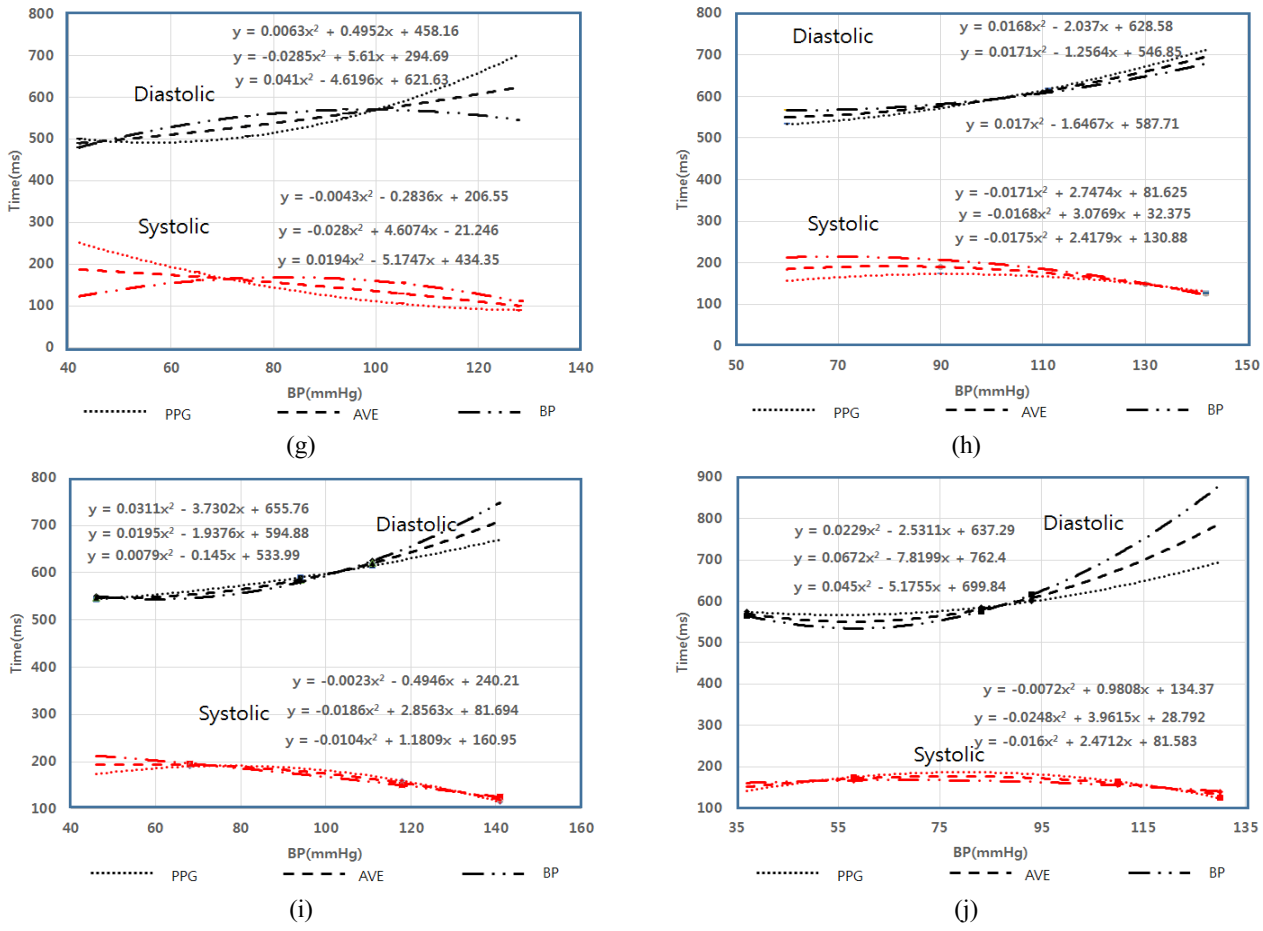


FIG. 8. Comparison of the time shifts (SRT, DFT) in the BP waveform and PPG data of subject A (Continue).

TABLE 4. Individual and averaged diastolic and systolic correlation coefficients obtained from the trend line between the time shifts of the BP waveform and the PPG data

| Subject | Diastolic correlation coefficient | Systolic correlation coefficient |
|---|---|---|
| A | 0.85 | 0.87 |
| B | 0.91 | 0.89 |
| C | 0.89 | 0.88 |
| D | 0.92 | 0.88 |
| E | 0.95 | 0.96 |
| F | 0.81 | 0.9 |
| G | 0.85 | 0.81 |
| H | 0.92 | 0.92 |
| I | 0.95 | 0.95 |
| J | 0.76 | 0.83 |
| Average | 0.881 | 0.889 |

fore, rather than using a BP waveform obtained with an inconvenient cuff, it is possible to use a PPG waveform obtained easily from the wrist.

Other researchers, seeking to estimate BP from the PPG SRT and DFT, have used representative trend curves created by plotting PPG time-shift peaks versus BP. Applying this conventional method to the data of Table 3, the single resulting trend line (created via linear regression of all SRT and DFT data) is shown in Fig. 9. Thus, the aim of the Fig. 9 is to show that the result of R using 10 subjects is lower than the correlation coefficient of peak shift and BP compared to each individual. Yun et al. [14] also experimented using multiple numbers of subjects, the result showed lower than the R value proposed in this method.

The correlation coefficients between the systolic and diastolic data were 0.4517 and 0.5060, respectively (thus essentially $\leq 0.5$), and the trend lines were opposite in terms of the slope.

However, again using the data of Table 3, Figs. 10(a)~10(j) show that the mean correlation coefficients of the individual trend lines were 0.921 for the SRT and 0.918 for the DFT (Fig. 10). Thus, the individual data are much more accurate. It is difficult to estimate BP using the conventional trend line.

### 3.3. Correlations Between PPG Signals and BP

The PPG and BP waveforms were very similar in all 10

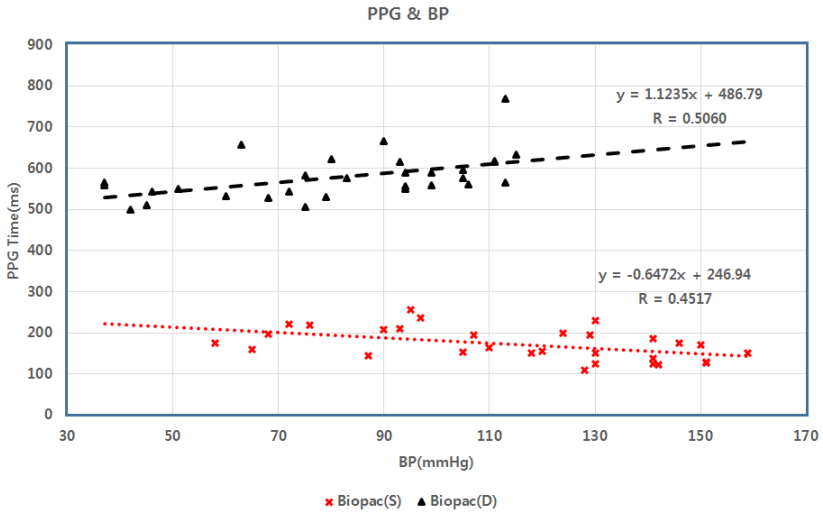


FIG. 9. Linear regression trend lines for the averaged PPG SRTs and DFTs of all subjects (red lines: SBPs; black lines: DBPs) (N=10).

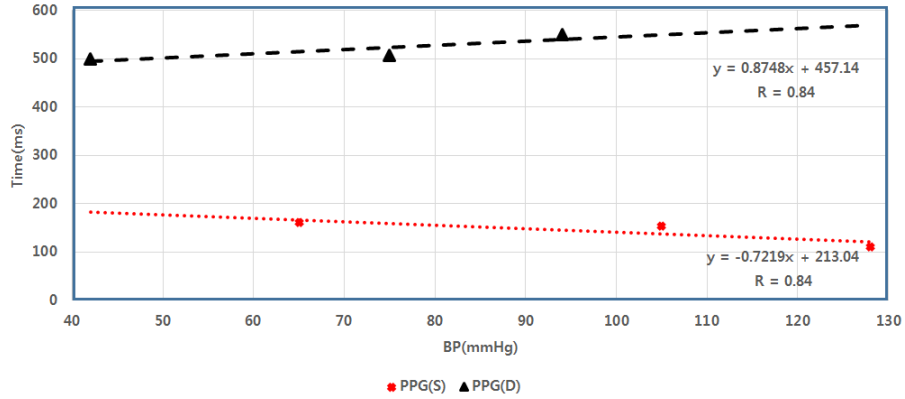


FIG. 10. Linear regression trend lines for the individual PPG SRT and DFT data obtained from subject A one time measured (red line, SBP; black line, DBP).

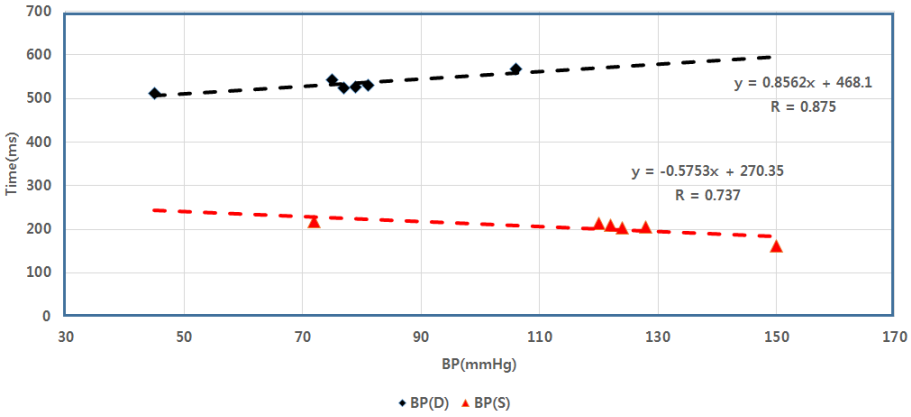


FIG. 11. Linear regression trend lines of the PPG SRT and DFT data obtained from subject K over 3 days (red line, SBP; black line, DBP).

subjects. To confirm reproducibility, a further six subjects were assessed, and data were obtained on 3 separate days. Figure 11 shows that the mean correlation coefficients between the PPG SRT and DFT data were 0.86 and 0.74, respectively. These values were lower than those obtained previously (DFT, 0.918; 0.921, SRT). However, the indi-

vidual correlation coefficients were higher than the average coefficients (SRT, 0.4517; DFT, 0.5060). The mean correlation coefficients of the 3-day data were higher than those of Yoon et al. [14] (0. SRT, 6050; DFT, 0.764). Therefore, our BP measurements were more accurate.

## IV. CONCLUSION

We explored the relationships among BP, compliance, and the PPG peak time shifts using a two-compartment Windkessel model of blood vessels. The RLC parameters of the model were estimated from sample BP waveforms, and their validities were confirmed using PSpice simulation. As the BP increased, the SRT fell with decreasing compliance, and rose when compliance increased. Simultaneous measurement of BP wave and PPG parameters under various BP conditions showed that the SRTs and DFTs yielded by the approaches showed an inverse pattern of change according to BP variation. The PPG SRTs and DFTs estimated BP accurately in individual regression analyses. We plotted individual trend curves using the data obtained at each of three arm positions. The trend curves reflect changes in blood vessel compliance. PPG waveforms are easy to obtain such that continuous BP measurement is possible.

## ACKNOWLEDGMENT

This research was supported by the Kyungpook National University Bockhyeon Research Fund, 2015.

## REFERENCES

1. P. W. F. Wilson, R. B. D'Agostino, D. Levy, A. M. Belanger, H. Silbershatz, and W. B. Kannel, "Prediction of coronary heart disease using risk factor categories," Circulation **97**(18), 1837-1847 (1998).
2. B. P. M. Imholz, G. A. Van Montfrans, J. J. Settels, G. M. A. Van Der Hoeven, J. M. Karemaker, and W. Wieling, "Continuous non-invasive BP monitoring: reliability of Finapres device during the Valsalva manoeuvre," Cardiovasc. Res. **22**(6), 390-397 (1988).
3. A. Groppelli, S. Omboni, G. Parati, and G. Mancia, "Evaluation of noninvasive BP monitoring devices Spacelabs 90202 and 90207 versus resting and ambulatory 24-hour intra-arterial BP," Hypertension **20**(2), 227-232 (1992).
4. C. C. Poon and Y. T. Zhang, "Cuff-less and noninvasive measurements of arterial BP by pulse transit time," Conf. Proc. IEEE Eng. Med. Biol. Soc. **6**, 5877-5880 (2005).
5. S. Ye, G.-R. Kim, D.-K. Jung, S. Baik, and G. Jeon, "Estimation of systolic and diastolic pressure using the pulse transit time," World Acad. Sci., Eng. Technol. **4**(7), 303-308 (2010).
6. L. A. Geddes, M. H. Voelz, C. F. Babbs, J. D. Bourland, and W. A. Tacker, "Pulse transit time as an indicator of arterial blood pressure," Psychophysiology **18**(1), 71-74 (1981).
7. R. A. Payne, C. N. Symeonides, D. J. Webb, and S. R. J. Maxwell, "Pulse transit time measured from the ECG: an unreliable marker of beat-to-beat blood pressure," J. Appl. Physiol. **100**(1), 136-141 (2006).
8. V. Mouradian, A. Poghosyan, and L. Hovhannisyan, "Non-invasive continuous mobile blood pressure monitoring using novel PPG optical sensor," IEEE Top. Conf. Biomed. Wireless Technol., Networks, Sens. Syst., pp. 60-62 (2015).
9. K. Czuszynski, "Noninvasive evaluation of cardiac output based on various biosignals," Ph.D. Interdiscip. J., pp. 115-124.
10. Y. Kurylyak, F. Lamonaca, and D. Grimaldi, "A neural network-based method for continuous blood pressure estimation from a PPG signal," IEEE Int. Instrum. Meas. Technol. Conf. (I2MTC), pp. 280-283 (2013).
11. G. Fortino and V. Giampà, "PPG-based methods for non invasive and continuous blood pressure measurement: an overview and development issues in body sensor networks," IEEE Int. Workshop Med. Meas. Appl. (MeMeA), pp. 10-13 (2010).
12. X. F. Teng and Y. T. Zhang, "Continuous and noninvasive estimation of arterial BP using a photoplethysmographic approach," in *Proc. 25th Annual Inter. Conf. IEEE Eng. Med. Biol. Soc.* (Cancun, Mexico, 2003) pp. 3153-3156.
13. S.-H. Woo, Y. Y. Choi, D. J. Kim, F. Bien, and J. J. Kim, "Tissue-informative mechanism for wearable non-invasive continous BP monitoring," Sci. Rep. **4**, 1-6 (2014).
14. Y. Yoon and G. Yoon, "Nonconstrained BP measurement by photoplethysmography," J. Opt. Soc. Korea **10**(2), 91-95 (2006).
15. R. Samria, R. Jain, A. Jha, S. Saini, and S. R. Chowdhury, "Noninvasive cuffless estimation of BP using photoplethysmography without electrocardiograph measurement," IEEE Reg. 10 Symp., 254-257 (2014).
16. M. Elgendi, "On the analysis of fingertip photoplethysmogram signals," Curr. Cardiol. Rev., 14-25 (2012).
17. N. Westerhof, J. W. Lankhaar, and B. E. Westerhof, "The arterial Windkessel," Med. Biol. Eng. Comput. **47**(2), 131-141 (2009).
18. K. H. Wesseling, J. R. Jansen, J. J. Settels, and J. J. Schreuder, "Computation of aortic flow from pressure in humans using a nonlinear, three-element model," J. Appl. Physiol. **74**(5), 2566-2573 (1993).
19. N. Stergiopulos, B. E. Westerhof, and N. Westerhof, "Total arterial inertance as the fourth element of the Windkessel model," Am. J. Physiol. H81-H88 (1999).
20. P. Segers, A. Qasem, T. De Backer, S. Carlier, P. Verdonck, and A. Avolio, "Peripheral "oscillatory" compliance is associated with aortic augmentation index," Hypertens. **37**(6), 1434-1439 (2001).
21. O. Frank, "Die grundform des arteriellen pulses," Z. Biol. **37**, 483-526 (1899).
22. R. M. Goldwyn and T. B. Jr. Watt, "Arterial pressure pulse contour analysis via a mathematical model for the clinical quantifcation of human vascular properties," IEEE Trans. Bio-Med. Eng. **14**(1), 11-17 (1967).
23. Y. H. Ha, "Analysis of arterial blood pressure and its electrical analog model," Kyungpook National University Library, pp. 1-30 (1978).